Environ Sci Pollut Res (2017) 24:8825–8836
DOI 10.1007/s11356-017-8536-1

RESEARCH ARTICLE

An assessment of strontium sorption onto bentonite buffer material in waste repository

Pankaj Pathak[1,2]

Received: 29 August 2016 / Accepted: 31 January 2017 / Published online: 18 February 2017

Abstract In the present study, changes occurring in sorption characteristics of a representative bentonite (WIn-BT) exposed to $SrCl_2$ (0.001–0.1 M) under the pH range of 1–13 were investigated. Such interaction revealed a significant variation in surface charge density and binding energy of ions with respect to bentonite, and alteration in their physicochemical properties viz., specific surface area, cation exchange capacity, thermal and mechanical behaviour were observed. The distribution coefficients (k_d) calculated for sorption onto virgin (UCBT) and contaminated bentonite (CBT) indicated a greater influence of mineralogical changes occurred with variance of pH and strontium concentration. Notably, the sorption mechanism clearly elucidates the effect of structural negative charge and existence of anionic metal species onto CBT, and depicted the reason behind significant k_d values at highly acidic and alkaline pH. The maximum k_d of UCBT and $CBT_{(0.001M\ SrCl2)}$ were 8.99 and 2.92 L/kg, respectively, at the soil pH 8.5; whereas it was 2.37 and 1.23 L/kg at pH 1 for the $CBT_{(0.1M\ SrCl2)}$ and $CBT_{(0.01M\ SrCl2)}$, respectively. The findings of this study can be useful to identify the physicochemical parameters of candidate buffer material and sorption reversibility in waste repository.

Responsible editor: Georg Steinhauser

Electronic supplementary material The online version of this article (doi:10.1007/s11356-017-8536-1) contains supplementary material, which is available to authorized users.

✉ Pankaj Pathak
pankajpathak18@gmail.com

[1] Department of Environmental Science and Engineering, Marwadi Education Foundation, Gauridad, Rajkot, Gujarat 360003, India

[2] Department of Civil Engineering, Indian Institute of Technology (IIT) Bombay, Powai, Mumbai -400076, India

Keywords Strontium · Bentonite · Buffer material · Distribution coefficient · Sorption mechanism

Introduction

^{90}Sr, the β-emitter radionuclide with a half-life of 28.8 years, average biological half-life ~18 years and decay energy 546 KeV, is the foremost isotope of strontium (Alfredo et al. 2014; Glasstone and Dolan 1977; Guimaraes et al. 2014; IAEA 2006; Keceli 2015; Smiciklas et al. 2015). The significant amounts of ^{90}Sr radionuclides produced from nuclear reactors and/or fallout from weapon testing remained in the spent fuels were identified as a serious threat to the sustainable world (IAEA 2006; Mckinley et al. 2007; Zhijian 2008). The mobility of radiation emitted by nuclear wastes (containing strontium isotopes) can only be prevented by their decay and decontamination. For this, deep geological disposal has remained in-practice wherein the radioactive wastes are kept prolonged in isolation in the multi-barrier repository (IAEA 2006; Zhijian 2008).

In such repositories, bentonite has remained a prime candidate buffer material, often surrounded by the packaging material either of concrete at low pH < 4 or cement at high pH > 10 (IAEA 2006; Kwon et al. 2013; Mckinley et al. 2007; Till and Grogan 2008; Zhijian 2008). Owing to the exceptional characteristics of high swelling potential, low permeability, self-sealing capacity, higher cation exchange capacity, specific surface area and active mineralogy, the bentonite exhibits high sorption capacity (commonly determined as a distribution coefficient, k_d) to facilitate the proper functioning of waste repository (Caglar et al. 2009; Mckinley et al. 2007; Zhijian 2008). The development of engineered multi-barrier waste repositories was pioneered albeit the adversity caused by natural and/or manmade intrusion, due to potential leakage

in waste packaging, fire/explosion by the excessive pressure build-up inside the container, which would result in damage to the repository (IAEA 2006; Mckinley et al. 2007). This situation may lead to direct contact between the bentonite buffer material and acidic/alkaline pore fluid of radioactive wastes. In the past, fluid leakage from repositories had led to severe ^{90}Sr contamination in soils/sediments/groundwater at a number of sites worldwide, including Hanford, New Mexico and Oak-Ridge (USA), Mayak in Russia and Fukushima in Japan (Kamei-Ishikawa et al. 2013; Keceli 2015; Wallace et al. 2012). Moreover, the solid strontium gets solubilized in water and may cause a serious threat to human health. Therefore, its limit in drinking water has been restricted to 1.5 ppm with an average annual drinking water limit of 182.8 mCi ^{90}Sr (IAEA 2006; Gllowiak et al. 1977). Exposures above the permissible limit have chronic effects on the human body which can lead to somatic and genetic changes, and further develop several types of cancer in the bone, nose, lungs and skin (IAEA 2006; Smiciklas et al. 2015).

Therefore, with a necessity to understand the possible failure of a multi-barrier repository system, the relative changes in bentonite properties (before and after strontium contamination) should be investigated. Though the previous studies revealed that the longevity of bentonite buffer material primarily depends on the mineral contents, pH of pore solution and the temperature generated within the repository (IAEA 2006; Guimaraes et al. 2014; Guven 1990), it was observed that sorption properties of bentonite-contaminant interaction were substantially influenced by the physicochemical properties (i.e. cation exchange capacity, CEC; specific surface area, SSA; pH), the contaminant properties (i.e. pH, type and concentration of ionic species) and the mineralogy of bentonite (\Arnepalli et al. 2010; Guven 1990; Karnland et al. 2007; Pathak 2014; Pathak et al., 2014a, b, 2015). A greater influence on sorption onto bentonite was observed when the isomorphic substitution occurred in tetrahedral sheets by replacing tetravalent with trivalent ions and in octahedral sheets by the replacement of trivalents with divalent ions (He et al. 2016; Seliman et al. 2014); whereas, the nano-porous iron oxyhydroxides of large surface area (Srivastava et al., 2012, 2013) in bentonite often supports the phenomena for *outer*-sphere cation exchange (Wallace et al. 2012). Notably, previous studies on strontium sorption dealt with virgin bentonite and none of them determined the subsequent effect of contamination onto the contaminated bentonite soil (CBT). Therefore, such study would be helpful to understand the changes occurring in sorption properties of the bentonite buffer material in repositories, and sorption reversibility of the contaminated bentonite at the time of adversity. The need of this investigation can be underlined as the ^{90}Sr in buffer material forms weakly bound surface complexes, which may be remobilized to a substantial extent if the ionic strength of groundwater increases or, with any saline intrusion.

Moreover, the present piece of work would be more relevant in a current scenario of India's civil nuclear energy program with a flourishing target of 24 GW by 2030 from the present capacity of ~6 GW (India Energy Outlook 2015). This would unprecedentedly generate the large amount of radionuclide wastes to fulfil the clean energy requirements for the rapid industrialization and economic growth of India. Hence, the search for suitable buffer (bentonite) material is ongoing, and one such plausible sample (WIn-BT) was used in this study. The present paper deals with a systematic study on the significant changes occurring in bentonite properties due to the acidic and alkaline attack of strontium.

Experimental investigation

A commercially available bentonite, WIn-BT, collected from the western part of India was used in this study. To simulate the contamination onto bentonite buffer material in laboratory, the WIn-BT was exposed to a model contaminant (in non-radioactive form) solution of 0.1, 0.01 and 0.001 M $SrCl_2$. At a liquid-to-solid ratio, L/S = 5 where 20 g soil mixed with 100 ml of solution and stirred for 1 h, the pH (1, 4, 10, 13) of the uniform slurry was separately maintained by the addition of H_2SO_4/NaOH solution under stirring; the soil pH (without any acid/alkali addition) was nearly 8.5 (±0.2). After 1 h of mixing, the slurries were kept in closed containers for 30 days to dry. For an uncontaminated reference buffer material, WIn-BT was also mixed with distilled water and kept for 30 days. In this way, 15 types of contaminated bentonite soils designated as CBT and one uncontaminated bentonite soil designated as UCBT were prepared in the laboratory. The sorption reversibility of UCBT and CBT were subsequently studied in the laboratory by considering a similar contaminant ($SrCl_2$) at an initial pH of 6.5 for batch tests (Pathak et al., 2014a, b, 2015). A wide range of concentrations C_i = 0.7, 0.5, 0.4, 0.3, 0.2, 0.1, 5×10^{-2}, 1×10^{-2}, 5×10^{-3}, 1×10^{-3} and 1×10^{-4} M of $SrCl_2$ were selected, and the k_d values were computed by employing the Freundlich isotherm (Pathak 2014; Pathak et al., 2014a, b, 2015), which is used to describe the heterogeneous system (He et al., 2016), as presented in Eq. 1.

$$C_s = k_d \cdot \sqrt[n]{C_e} \quad (1)$$

where k_d is the distribution coefficient (in $g^{1-1/n}\,L^{1/n}kg^{-1}$), n is a constant accounted for soil heterogeneity and C_e (in g/L) and C_s (in g/kg) are the concentrations of the contaminant in solution at equilibrium and sorbed onto soil. The k_d and 1/n can be calculated from the intercept and slope of plot C_s versus C_e (discussed in the Results and discussions section). Notably, the values of 1/n obtained from the plot were ~1 showing linearity, henceforth unit of the k_d value can be taken as litre/kilogramme. The overall process of sample preparation and computation of the k_d values are outlined in Fig. 1.

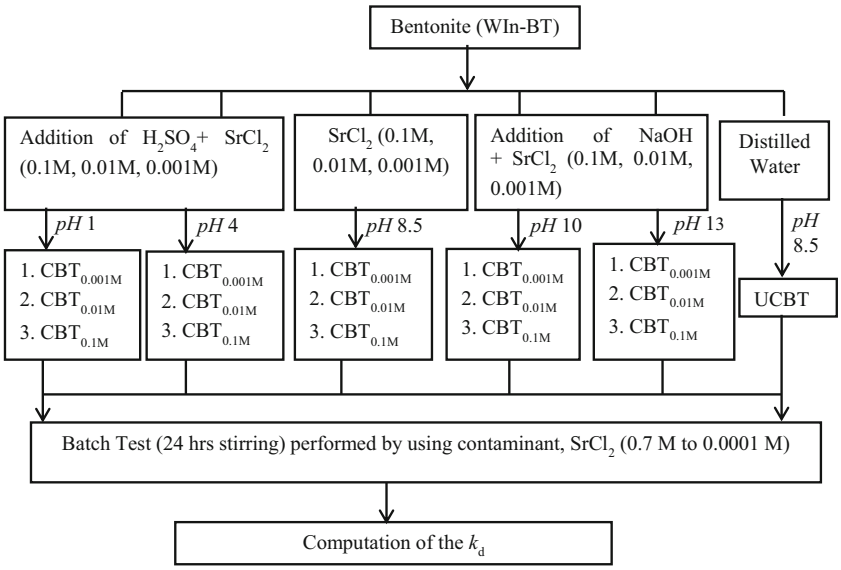

Fig. 1 A schematic flow sheet for preparation of UCBT, CBT and computation of the k_d

Physical characteristics of UCBT and CBT

The ASTM D 5550-06 guidelines(ASTM D 5550–06, 2008) were used for determination of specific gravity, *G*, of the soil by employing an ultra-pycnometer (Quantachrome, USA). Each experiment was performed in triplets, i.e. soil was analysed three times in the test and the average values are presented in Table 1.

Chemical, mineralogical and morphological characteristics of UCBT and CBT

A water quality analyser (Model PE 136, Elico Ltd., India) was used to acquire the chemical characteristics pH, electrical conductivity (σ) and total dissolved solid (*TDS*) of the UCBT and CBT at L/S = 20 (as shown in Table 1). Notably, σ and pH of distilled water were measured to be 4.88 μS/cm and 7.0 ± 0.2, respectively, at 25 °C. The ethylene glycol monoethyl ether (EGME) method was adopted to determine the SSA (in m^2/g) of UCBT and CBT in two replicates, as follows:

$$\mathrm{SSA} = W_a(0.000286W_s)^{-1} \quad (2)$$

where, W_a is the amount of EGME adsorbed on the soil (in g) and W_s is weight of the dry soil (in g). An average of the obtained results of SSA is listed in Table 1. Whereas the CEC of soil is indicative of type of ions sorbed onto it, their

Table 1 The properties of the soil-contaminant system

Soil + solution	Concentration (M)	pH (±0.2)	σ (mS/cm)	TDS (ppt)	*G*	SSA (m^2/g) × 10^2	ζ (mV)
UCBT	0	8.4	1.24	0.66	2.45	5.55	−24.80
Soil + H_2SO_4 + $SrCl_2$	10^{-3}	1	51.55	20.75	2.26	4.14	1.84
	10^{-2}		54.55	21.89	2.31	4.24	2.53
	10^{-1}		58.16	23.44	2.42	4.85	10.07
	10^{-3}	4	2.63	1.32	2.55	5.52	−28.73
	10^{-2}		4.15	20.72	2.49	5.49	−25.33
	10^{-1}		18.82	9.39	2.54	5.16	−8.36
Soil + $SrCl_2$	10^{-3}	8.5	1.50	0.75	2.45	5.25	−30.93
	10^{-2}		3.42	1.71	2.46	5.19	−26.16
	10^{-1}		18.84	9.41	2.54	4.83	−8.86
Soil + NaOH + $SrCl_2$	10^{-3}	10	1.50	0.75	2.51	5.22	−33.23
	10^{-2}		3.59	1.79	2.41	4.59	−30.80
	10^{-1}		18.94	9.45	2.37	4.28	−16.23
	10^{-3}	13	14.41	7.21	2.50	4.60	−29.63
	10^{-2}		19.45	9.72	2.51	4.40	−23.60
	10^{-1}		29.01	14.54	2.47	4.38	−7.55

Table 2 The cation exchange capacity of UCBT and CBT at different pH

S.N.	$CBT_{(M)}$	pH (±0.2)	CEC_{Na} (meq/100 g)	CEC_K	CEC_{Ca}	CEC_{Mg}	CEC_{Sr}	CEC_{Fe}	CEC_{Al}	CEC_{Total}
1	UCBT	8.5	120.5	0.3	4.6	1.7	–	0.2	0.4	127.6
2	10^{-3}	1	87.7	0.1	0.1	0.4	0.1	0.2	0.3	89.0
3	10^{-2}		80.7	0.2	0.7	0.4	6.9	5.1	0.2	94.1
4	10^{-1}		76.9	0.1	0.2	0.3	12.6	10.1	0.4	100.7
5	10^{-3}	4	132.1	0.3	0.7	0.8	–	0.2	0.3	134.4
6	10^{-2}		118.8	0.3	0.7	0.9	3.0	2.2	0.3	126.2
7	10^{-1}		92.2	0.2	0.4	0.8	2.5	3.5	0.3	99.7
8	10^{-3}	8.5	118.3	0.3	4.5	1.7	–	0.2	0.3	125.4
9	10^{-2}		93.7	0.2	8.0	1.3	3.1	8.6	0.3	115.2
10	10^{-1}		99.9	0.2	2.8	1.3	0.5	2.9	0.2	107.8
11	10^{-3}	10	118.7	0.3	5.3	1.7	1.2	0.2	0.2	127.6
12	10^{-2}		114.3	0.3	6.3	1.8	–	0.9	0.2	123.8
13	10^{-1}		75.7	0.2	1.3	0.8	6.1	4.4	0.4	89.1
14	10^{-3}	13	106.9	0.3	26.0	1.7	1.6	4.2	0.1	140.7
15	10^{-2}		115.8	0.3	19.7	1.2	10.9	8.4	0.2	156.5
16	10^{-1}		86.6	0.2	1.9	0.6	14.0	11.2	0.1	114.6

– not detected

replacement by other ionic species was determined by the sodium acetate method. For this, triplets of each sample were measured and their average is presented in Table 2.

The influence of contaminant on soil particles can be estimated by measuring its net surface charge or zeta potential (ζ), determined at L/S = 100 (results shown in Table 1) using an automated electrophoresis instrument Zeta PALS, BIC (USA). Chemical bonding in soil samples was identified by using the acquired spectra of Fourier transform infrared (FTIR; Model: MAGNA 550, USA), for which the KBr was used to prepare the soil sample pallets. Samples were analysed in the mid-IR range from 4000 to 400 cm^{-1} (spectra shown in online resource Fig. S1). The mineralogical characterization was carried out by using an X-ray diffraction spectrometer (Philips, Eindhoven, the Netherland) with Cu-Kα as a radiation source under a slow scan of 2 °/min (refer Fig. 2 and online resource Table ST1). The morphological characteristics of the soil samples were studied by an environmental scanning electron microscope (SEM; Quanta 200, FEI, Netherland) and the micrograph is presented in online resource Fig. S2.

Thermal and mechanical characteristics of UCBT and CBT

The thermal response of soil was observed by the thermo gravimetric and differential thermal analysis (TG-DTA) using a Perkin Elmer (USA) Diamond TG/DTA. Measurements of weight loss against the original input soil (20 mg for each sample) up to 600 °C were taken under isothermal heating in air (flow rate 50 mL/min) and a heating rate of 5 °C/min (results shown in online resource Fig. S3). The endothermic and exothermic behaviour were analysed via the recorded difference in temperature between soil sample and reference material (alumina), results shown in online resource Fig. S4.

The mechanical properties (viz., hardness, H and residual young's modulus, Er) of soil were determined by load-displacement relationships (Oyen and Cook 2009). A nanoindentation (Model TI 900 TriboIndenter, Hysitron, USA) experiment was performed on UCBT and CBT at three different loads of 1000, 2000 and 3000 μN (Srinivas et al. 2013). Subsequently, the hardness and residual modulus were calculated by Eqs. 3 and 4, respectively, as follows:

$$H = \frac{P}{A_c} \tag{3}$$

$$E_r = \frac{\sqrt{\pi}}{2\beta\sqrt{A_c}}S \tag{4}$$

where P is the applied load (in μN), A_c is the projected contact area between the indenter and the sample (in nm^2), π and β are dimensionless correction factors for the indenter tip shape and S is the contact stiffness.

Two different indentation area of each sample were selected and the numbers of indentations of each area were 12. The average result of 12 indentations of each area was shown as replicates I and II as given in online resource Table ST2. Further, to generalize the discrimination in soil heterogeneity, the average results of hardness and residual modulus of applied load taken at different concentrations of contaminated bentonite, are shown in Fig. 3.

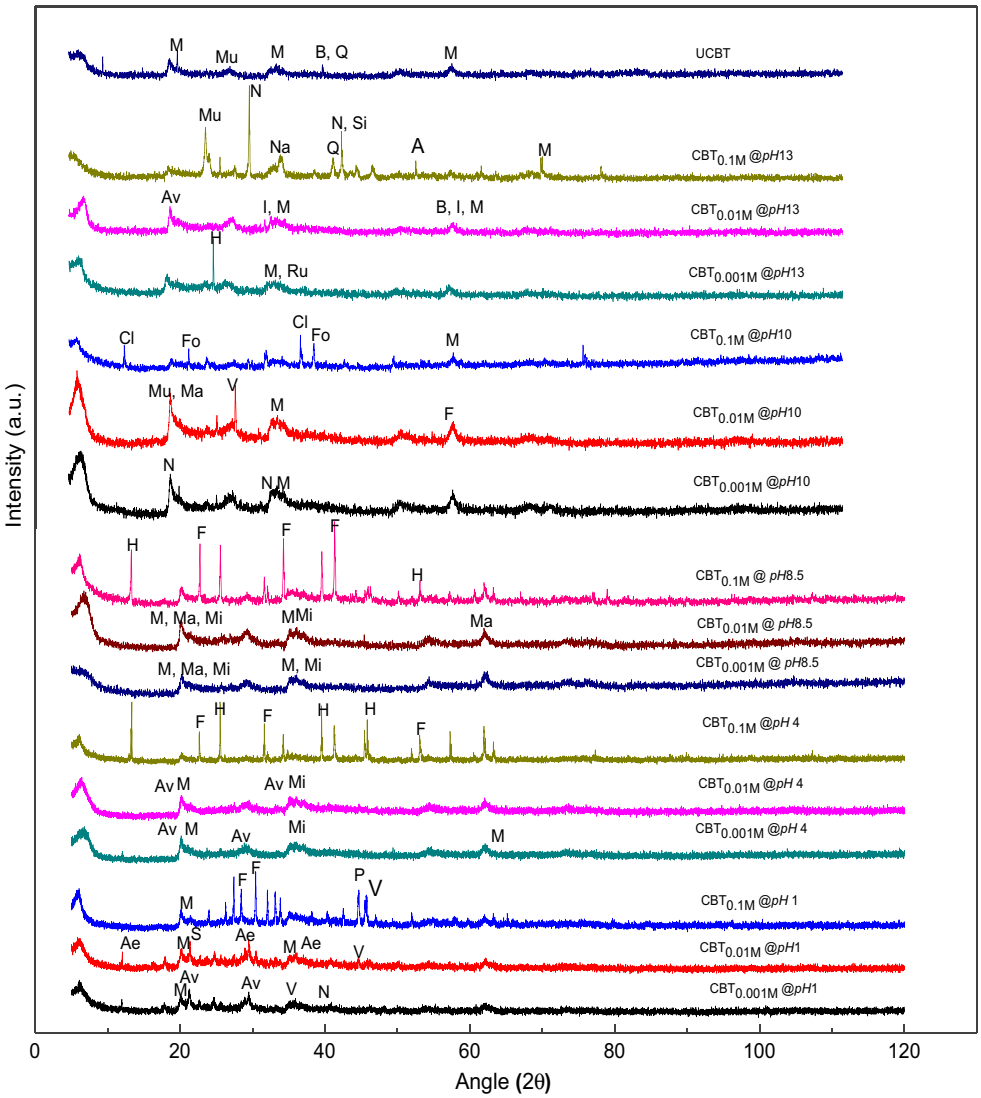

Fig. 2 The XRD diffractograms of CBT and UCBT at different pH. *Ae* aerinite, *Av* allevardite, *F* faujasite, *H* halite, *M* montmorillonite, *N* nontronite-15A, *I* illite, *P* periclase, *S* saponite, *Mu* muscovite, *Ca* cacoxenite, *Si* sillimanite, *A* anorthite, *Na* natrolite, *V* vermiculite, *Mi* mica, *Ma* magnetite, *Cl* clinochlore IIb-4, *Fo* forsteriteferroan, *B* beidellite-12A, *Ru* rutile

(Note: Ae-Aerinite, Av-Allevardite, F-Faujasite, H-Halite, M-Montmorillonite, N-Nontronite-15A, I-Illite, P-Periclase, S-Saponite, Mu-Muscovite, Ca-Cacoxenite, Si-Sillimanite, A-Anorthite, Na- Natrolite, V-Vermiculite, Mi-Mica, Ma-Magnetite, Cl-Clinochlore IIb-4, Fo-Forsteriteferroan , B-Beidellite-12A, Ru-Rutile)

Results and discussions

Effect of physicochemical-mineralogical properties

The cation exchange capacity (CEC) is one of the main factors, which has been considered for manifesting the number of ionic charges on soil particles and the sorption characteristics of soil-contaminant systems (Pathak et al., 2014a, b, 2015). A high CEC values results from the isomorphous substitution of Si^{4+} and Al^{3+} with low valance cations (Na^{+}, K^{+}, Ca^{2+}, Mg^{2+}) in the soil structure. Due to its larger SSA, the bentonite is a candidate buffer material (Caglar et al. 2009; Seliman et al. 2014). The context can easily be understood from Tables 1 and 2, as the characteristics of CBT such as G, SSA, CEC and ζ are greatly affected by the variance of pH and contaminant concentration. The soil characteristics as a function of contaminant concentration in CBT are shown in Fig. 4, which indicates that increasing concentration of contaminant in CBT (from 0.001 to 0.1 M $SrCl_2$) at pH ≥ 4 resulted in a decreasing G, SSA and CEC; on the contrary, soil properties tended to be enlarged with increasing CBT concentration at pH 1. Furthermore, the values of ζ were found to be ≤ ±30 mV which specified the soil suspensions were not stable; however, in $CBT_{(0.001MSrCl2)}$ at pH 10, ζ was −33.23 mV and displayed stable soil particles. The ζ determines an isoelectric point (IEP) and estimates the interaction between soil-contaminant solution as a function of pH and concentration of the electrolyte species (Duman and Tunc, 2009; Moayedi et al. 2011). Keeping this in view, pH vs. ζ relationship was plotted (refer online resource Fig. S5) and IEP (i.e. ζ = 0 mV, represent

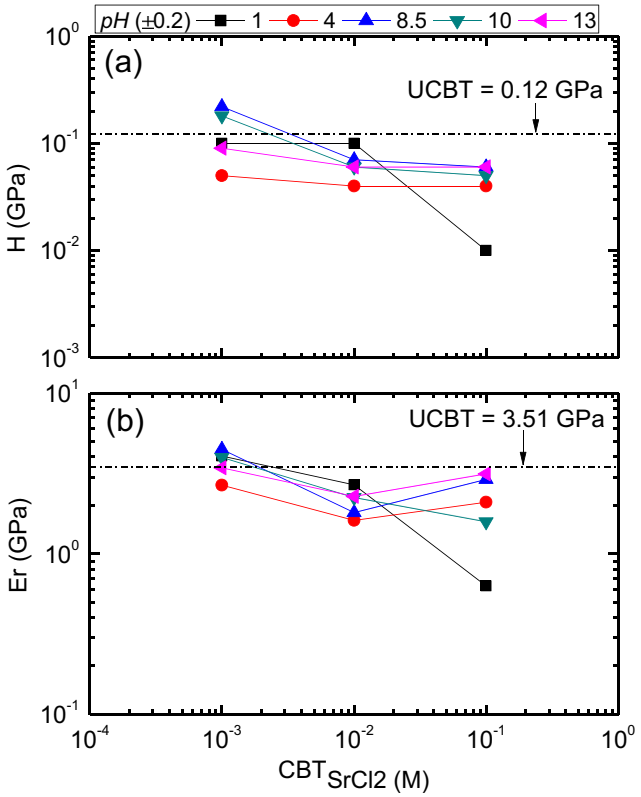

Fig. 3 The mechanical properties (**a**) Residual Young's Modulus and (**b**) hardness for CBT at different pH

neutral sites) were estimated at pH 1.2, 1.3 and 2.6 for $CBT_{(0.001MSrCl2)}$, $CBT_{(0.01MSrCl2)}$ and $CBT_{(0.1MSrCl2)}$, respectively. It was noticed that pH greater than IEP, the mobile counter ions $(AlO_4)^{5-}$, OH^- and $(MgO_4)^{6-}$ in the diffuse layer yielded negative ζ (refer Table 1). However, when pH decreases from IEP then surface charge on CBT get changed due to sorption of counter ions and displays screening ion effect. The ζ values +1.84 to +10.04 mV were obtained at pH 1 in consequence of H^+ and Sr^{2+} which sorbed on outer Helmholtz plane of the Stern layer. In the electrostatic field, these ions move towards slipping plane and alters the surface charge from negative to positive (Duman and Tunc, 2009; Wang et al. 2010). A further uptake of contaminant onto CBT could decrease the amount of protons by replacing with Sr^{2+}. In this circumstance, the surface active co-ions can move towards diffuse layer and revers the surface charge, which can be corroborated to the available sorption sites onto CBT.

The change in chemical bonding of UCBT after being contaminated can be discussed by analysing the FTIR spectra (refer online resource Fig. S1). A slight shift in peak position from 3348 to 3410 cm^{-1} from UCBT to CBT, respectively, corresponds to the OH stretching of H-bonded water. The change is due to the replacement of divalent Ca^{2+} and Mg^{2+} with Sr^{2+}. The band at 3604 cm^{-1} can be attributed to adsorbed water (stretching mode of hydroxyl group) and here mainly due to the Al─Al─OH and Al─Mg─OH (Caglar et al. 2009; Madejova 2003). A band at 1631 cm^{-1} corresponds to the bending mode of adsorbed water (H─O─H) in soil with

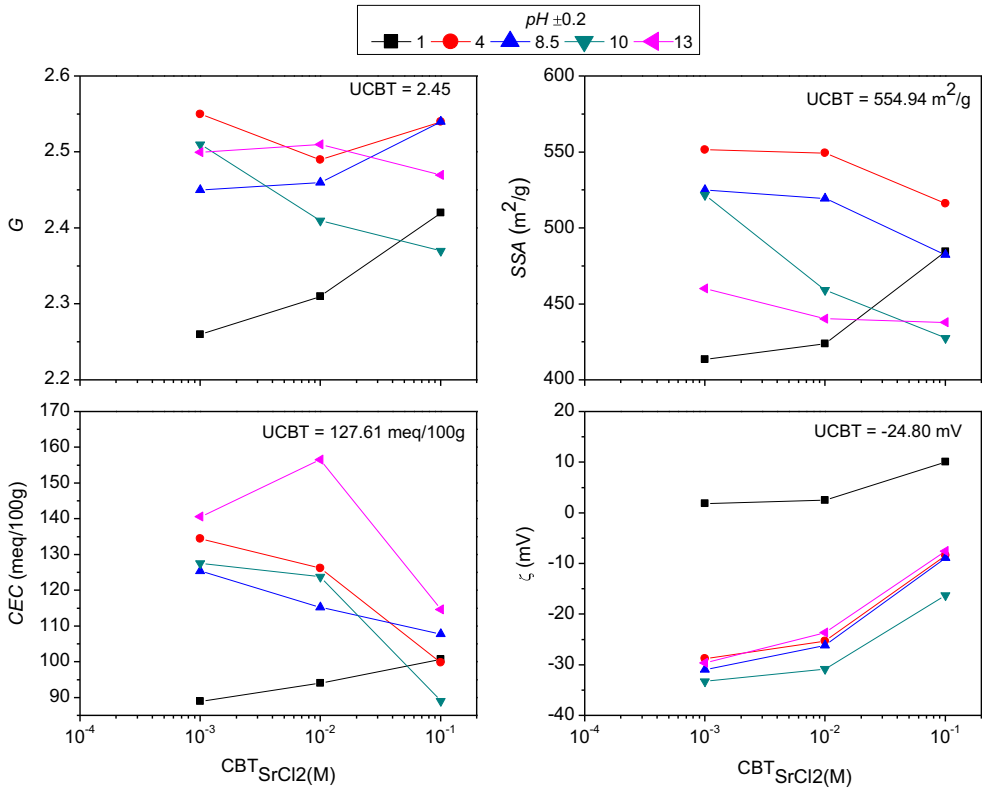

Fig. 4 The relationship between concentrations of $SrCl_2$ at CBT with soil characteristics, i.e. specific gravity, *G*; specific surface area, *SSA*; cation exchange capacity, *CEC* and zeta potential, ζ at different pH

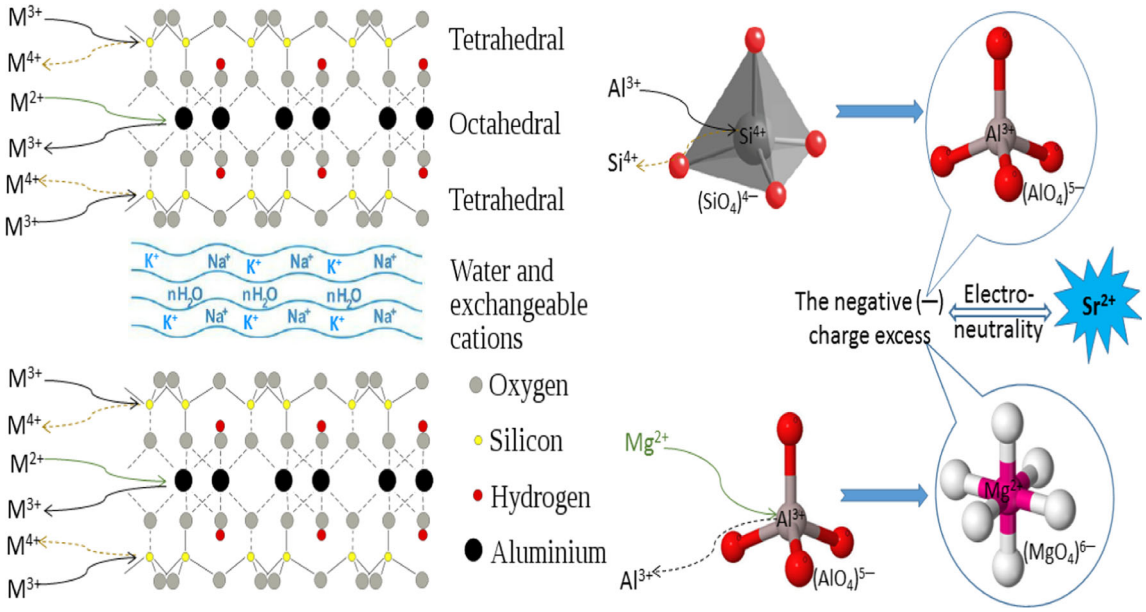

Fig. 5 A typical representation of sorption mechanism for the bentonite-strontium system

SiO_2/Fe_2O_3 minerals. The intensive peaks at 1024 and 520 cm^{-1} correspond to the vibration stretching of Si—O—Si and bending of Si—O—Al, respectively. The Fe—O vibrational bands were observed at 457 and 1484 cm^{-1}. The change in FTIR spectra of UCBT and CBT revealed the acidic and alkaline attack on bentonite which led to the alteration of mineralogical properties of bentonite and was further evident from XRD analysis (as shown in Fig. 2 and online resource Table ST1). The major mineral of UCBT was found to be montmorillonite (Seliman et al. 2014). The XRD analysis indicated that as the concentration of contaminant increased with pH, the degree of crystallinity of CBT also increased (Fig. 2). Further, at low concentration of $CBT_{(0.001M\ SrCl2)}$ and pH ≥ 4, slight changes were observed in the mineral phases. However, peaks of nontronite and allevardite were identified at pH 1. Nontronite is an iron-rich smectite mineral whose formation may have been facilitated by the iron content in the sample (refer Table 2). The formation of allevardite indicated the interstratified mica and montmorillonite layers in the structure. The mineralogical alteration observed in bentonite under the studied conditions clearly displayed the plausible changes in the sorption characteristics of bentonite (Guven 1990; Galambos et al., 2012).

Furthermore, the surface morphology of UCBT and CBT explain the arrangement of soil particles (online resource Fig. S2). Vertical rod-shaped particles (due to $SrSO_4$ and/or $SrCl_2$ crystals) on soil surfaces were observed at pH 1 with phase-to-phase arrangement in a dispersed manner. As pH increased from 4 to 10, the flocculated soil particles increases the repulsive forces between the soil surface and vary with the ζ value. Interestingly, at pH 13, the soil particles displayed a stratified flocculated structure. Hence, a decreased thickness of the diffuse double layer resulted in shrinking soil particles of CBT (Gumaste et al. 2014); consequently, increased specific gravity and reduced SSA were also observed (as presented in Table 1). This highlights the fact that contaminant exposure onto bentonite decreases the sorption capacity of CBT than that of the UCBT.

Effect of thermal and mechanical properties

The thermal stability of bentonite was investigated by thermogravimetric and differential thermal analyses (TG-DTA). The TGA graph (online resource Fig. S3) revealed rapid weight loss between 27 and 183 °C which was due to the loss of water molecules (Lalikova et al. 2010). A further increase in temperature up to 600 °C showed a slight weight loss due to dehydroxylation of organic compounds (Lalikova et al. 2010; Wendlandt 1975). This would indicate that the disposal of radioactive waste at higher temperature (>100 °C) may cause inertness and decrease the sorption capacity of bentonite. The two peaks in the temperature ranges 90–100 °C and 140–160 °C of the DTA curve (online resource Fig. S4) agree with the loss of water (Smykatz-Kloss 1982). The requirement of more energy above 400 °C is ascribed to the loss of hydroxyl ions from organic compounds, owing to the endothermic behaviour of soil. Thus, the organic compounds in the soil were degraded at elevated temperature (>400 °C), and which led to a decrease in sorption.

Further, the results of nanoindentation experiments revealed substantial changes in mechanical properties (hardness and residual Young's modulus) of CBT and UCBT (online resource Table ST3). Hardness and residual Young's modulus of UCBT are represented as horizontal dotted lines, i.e. 0.12

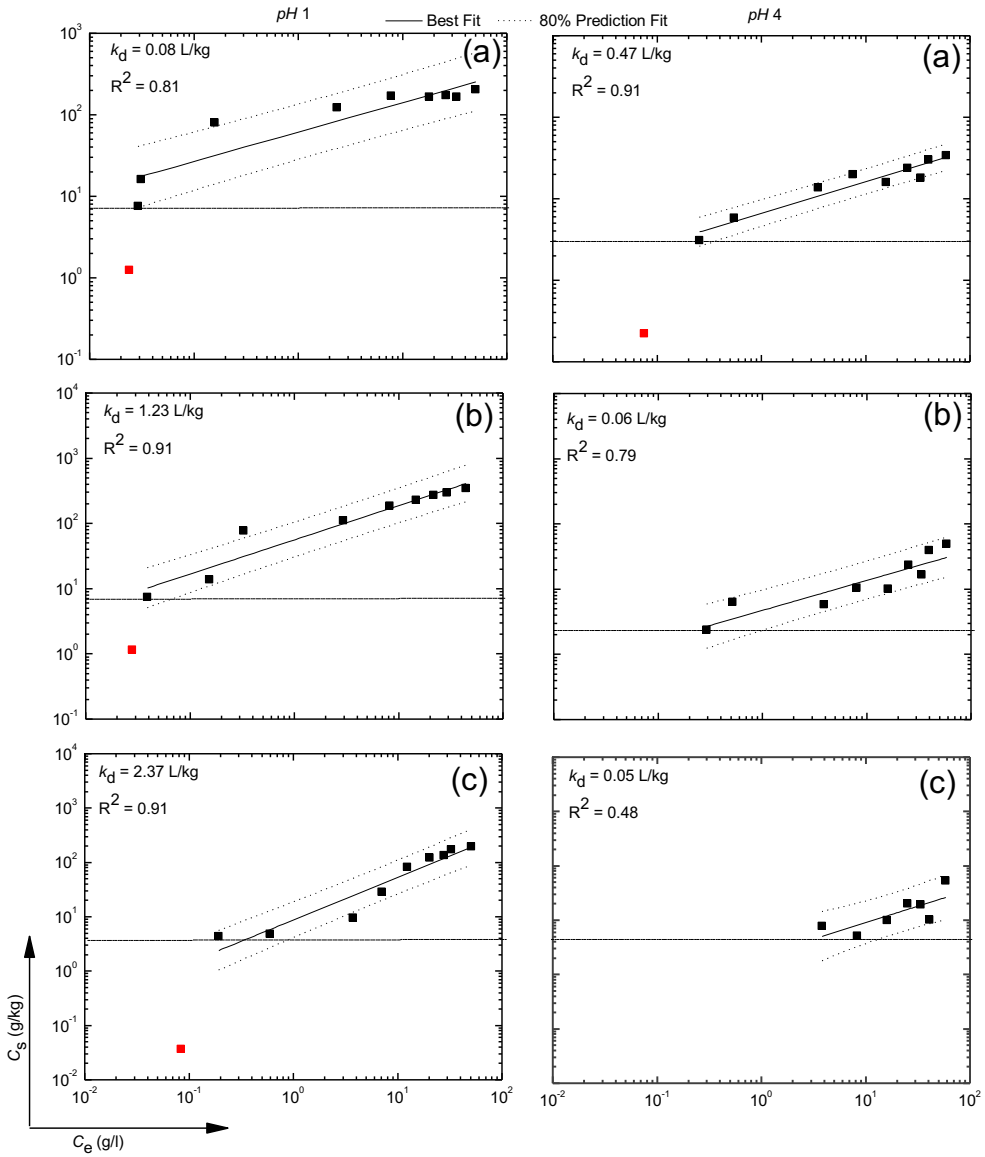

Fig. 6 The distribution coefficients for CBT-$SrCl_2$ system at pH 1 and 4 **a** 0.001 M, **b** 0.01 M and **c** 0.1 M

and 3.51 GPa, respectively, in Fig. 3a, b. It can be concluded that the hardness and residual stress of CBT decreased with an increased concentration of contaminant from 0.001 to 0.1 M, thus reducing the binding energy of ions present in CBT, might be responsible for alteration in SSA and CEC values. Moreover, an increase in binding energy can break the ionic bonds (Parkhomenkho 1967). Moreover, the hardness of the material was highly dependent on its phases viz., crystalline and amorphous (Hancock et al. 2002). The crystalline phase of CBT demonstrated by the sharp peaks of XRD (Hancock et al. 2002) as shown in Fig. 2 was more prominent with 0.1 M strontium contaminant which resulted in a substantial decrease in hardness (Fig. 3a). The hardness of the crystalline phase was less than in the amorphous phase of materials. Furthermore, the residual modulus (E_r) corresponding to the resilient stress in bentonite (Oliver and Pharr 1992) was subjected to effects of contaminant at different pH and concentrations. At pH 1 and 10, the E_r decreased with an increased $SrCl_2$ concentration. However, remaining CBT at pH 4, 8.5 and 13 exhibited stress randomness where E_r values decreased from 0.001 to 0.01 M, and increased for 0.1 M $SrCl_2$ (Fig. 3b). Based on this, the alteration in soil properties occurs at higher to lower concentration of contaminants. Such an alteration can be attributed to the variation in elasto-plastic behaviour of soil (Oliver and Pharr 1992), mainly due to the chemical attack onto soil at different pH.

Effect of soil properties on sorption mechanism

The minerology of bentonite significantly affects the sorption mechanism of the bentonite-contaminant system. As can be seen from Fig. 5, the octahedral Al^{3+} and

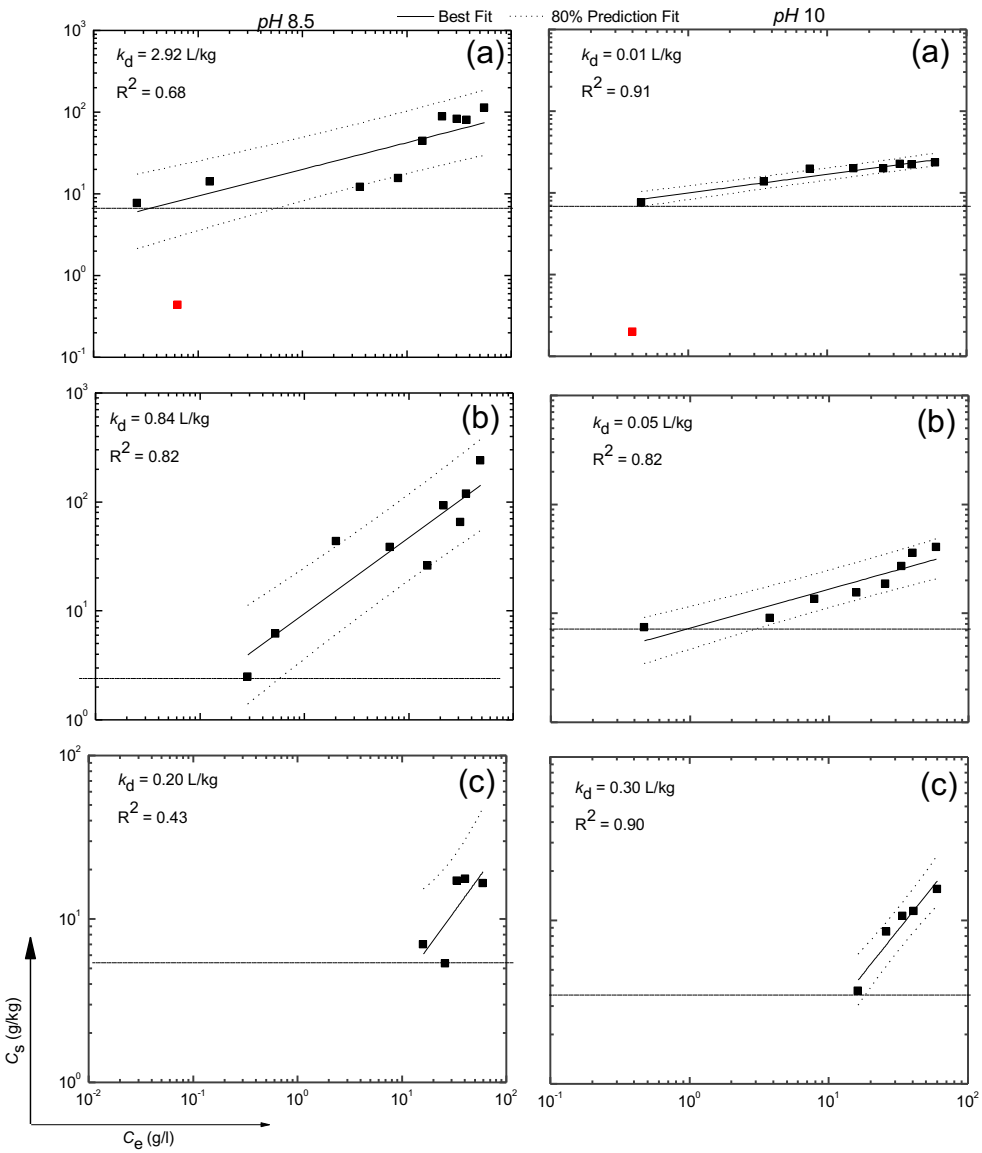

Fig. 7 The distribution coefficient for CBT-$SrCl_2$ system at pH 8.5 and 10 **a** 0.001 M, **b** 0.01 M and **c** 0.1 M

tetrahedral Si^{4+} sheets of the bentonite mineral are interacted by the isomorphous substitution of higher valence cations with the lower valences. These substitutions create a negative charge excess for the unsatisfied valences (Poernomo 2010; Seliman et al. 2014). Subsequently, the strontium (as Sr^{2+}) gets sorbed by the replacement of exchangeable cations (commonly the Na^+, K^+ and Ca^{2+}) and via ion-pairing with the negative charge excess created by anionic $(AlO_4)^{5-}$ and $(MgO_4)^{6-}$ (as shown in Fig. 5). This leads to chemisorption; however, physisorption via *outer*-sphere complexation of Sr^{2+} onto bentonite surface can also take place (Wallace et al. 2012; Poernomo 2010). Notably, the net negative charge excess compensated by metal cations (including Sr^{2+}) establishes the electroneutrality onto bentonite surfaces.

Nevertheless, the CBT further exposed to contaminant ($SrCl_2$) solution at different concentrations also revealed some other phenomena. Figures. 6, 7 and 8 showed the relationship between C_s verses C_e at different pH and types of CBT. The concentration range above the horizontal dotted line indicated the contribution of contaminant for quantifying the k_d in a soil-contaminant system, whereas below that line, sorption reversibility due to a salting-*in* effect took place which is also known as desorption (Pathak et al. 2015). The $CBT_{(0.1M\ SrCl2)}$ contacted with 0.1–0.7 M contaminant solution exhibited the sorption quite well, however, by contacting a lower contaminant solution (i.e. <0.1 M $SrCl_2$, the increased concentration of contaminant in the solution) at equilibrium was an evidence for sorption reversibility or desorption. A continuing trend was also observed from Figs. 6, 7 and 8 for the 0.01 and

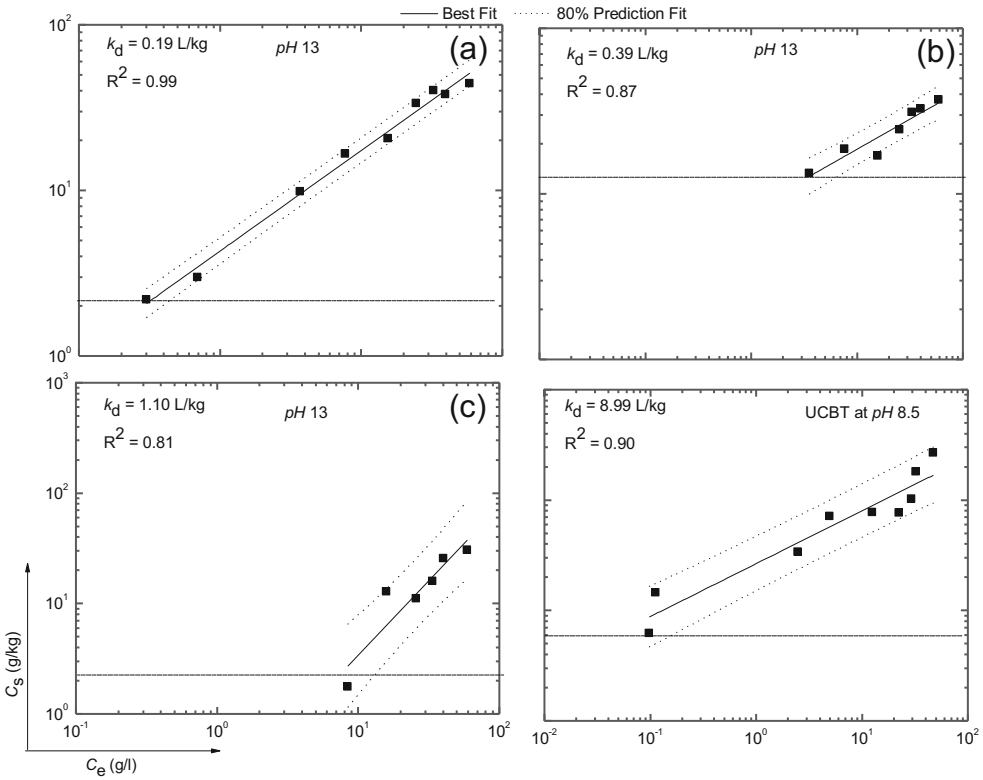

Fig. 8 The distribution coefficient for CBT-$SrCl_2$ system at pH 13 and UCBT-$SrCl_2$ at 8.5 **a** 0.001 M, **b** 0.01 M and **c** 0.1 M

0.001 M concentration of CBT. Figures 6a and 8a demonstrated that at pH 1, $CBT_{(0.1M\ SrCl2)}$ and $CBT_{(0.01M\ SrCl2)}$ displayed a greater k_d as compared to the $CBT_{(0.001M\ SrCl2)}$. The fact to be emphasized is that commonly at a lower pH, the protonation of specific sorption sites onto bentonite surface prevents the electrostatic sorption of Sr^{2+} (Wallace et al. 2012; Krauskopf and Bird 1995). This phenomenon clearly describes the insignificant k_d at pH 4. In contrast, the high k_d value at pH 1 can be corroborated with the permanent structural negative charges in clay minerals (Chen and Hayes 1999; Coppin et al. 2002; Parkman et al. 1998) and the presence of vermiculite (Langley et al. 2009; Wang et al. 2010). Additionally, precipitates of $SrSO_4$ co-exist with $CBT_{(0.1M\ SrCl2)}$ at pH 1 but redissolved when contacted with the contaminant solution, and thus, yielded a high k_d value. Subsequently, the sorption k_d = 2.92 L/kg of $CBT_{(0.001M\ SrCl2)}$ at pH 8.5 was consistent with the maximum sorption observed for Sr^{2+} on soil ascribed to the contribution of anionic hydroxyls (Wallace et al. 2012). The lower k_d values obtained for the $CBT_{(0.01M\ SrCl2)}$ and $CBT_{(0.1M\ SrCl2)}$ clearly indicated the effect of concentration (Wallace et al. 2012; Pathak et al. 2015). At alkaline pH 10, the addition of NaOH to fix the pH creates a significant area of uncertainty for the distribution of Na^+ between the interlayer and interparticle space (Galambos et al. 2012), and therefore may have decreased the k_d value. Interestingly, on further increase in pH up to 13, the k_d value for $CBT_{(0.1M\ SrCl2)}$ comparatively increased, which can be attributed to the anionic metal species onto bentonite surfaces. A plot for the k_d of CBT at varied concentrations as a function of pH is presented in Fig. 9. It revealed that the $CBT_{(0.001M\ SrCl2)}$ exhibited a higher k_d (2.92 L/kg) value at soil pH 8.5 though $CBT_{(0.01M\ SrCl2)}$ has a maximum k_d (1.23 L/kg) at acidic pH 1. On the other hand, the $CBT_{(0.1M\ SrCl2)}$ showed higher k_d at the extreme acidic and alkaline conditions as well (i.e. 2.37 L/kg at pH 1 and 1.10 L/kg at pH 13).

For an ideal candidate buffer material, the capacity to uptake contaminant/s is one of the prime factors to be determined

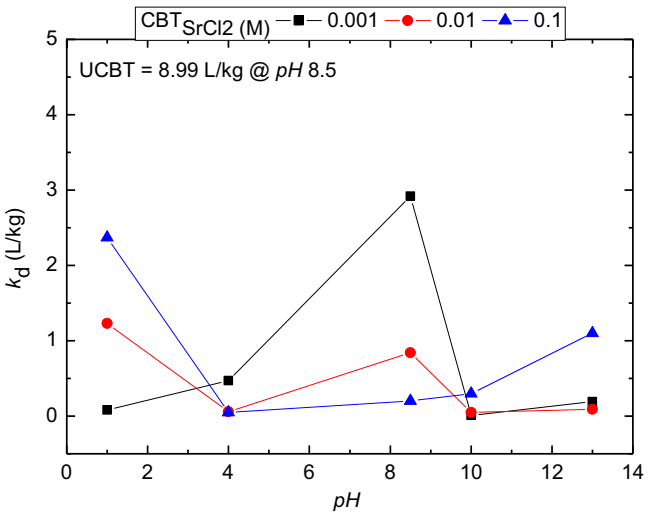

Fig. 9 The correlation of the distribution coefficient of CBT with respect to pH

along with the characteristics of sorbent material. Hence, the calculated sorption capacity of strontium onto the investigated samples was compared with other sorbents viz. activated charcoal, GMZ bentonite and local soil as reported in the literature (Chegrouche et al. 2009; He et al. 2016; Chegrouche et al. 2009; Hong et al., 2016). Notably, it was found that at soil pH, the sorption capacity of UCBT, i.e. 5.51×10^{-3} mol/m^2 was well in the range as compared to other sorbents such as activated charcoal 5.71×10^{-3} mol/m^2, GMZ bentonite 1.94×10^{-2} mol/m^2 and local soil 1.50×10^{-6} mol/m^2 (Chegrouche et al. 2009; He et al. 2016; Skupinski and Solecki 2014). It has been demonstrated that WIn-BT can be used as a potential buffer material in waste repositories.

Conclusions

Sorption properties of bentonite (WIn-BT) changed quite substantially due to the acidic and alkaline attack of strontium. The study revealed that sorption was highly influenced by the mineralogical changes that occurred due to pH variation, as well as changes in surface charge density, binding energy of ions and strontium concentration. Spectral and thermal analysis of the UCBT and CBT at varied pH and concentrations of $SrCl_2$ clearly demonstrated the alteration in soil properties. Due to the contaminant exposure to soil, substantial changes in the k_d values of UCBT and CBT were quantified. The maximum k_d of UCBT and $CBT_{(0.001M\ SrCl2)}$ at soil pH 8.5 were 8.99 and 2.92 L/kg, respectively; whereas for $CBT_{(0.1M\ SrCl2)}$ and $CBT_{(0.01M\ SrCl2)}$, the maximum k_d 2.37 and 1.23 L/kg, respectively, were obtained at acidic pH 1. A significant k_d value (1.10 L/kg) observed at pH 13 for $CBT_{(0.1M\ SrCl2)}$ was due to the ion-pairing of Sr^{2+} with the anionic metal species onto bentonite. Based on the experimental findings, WIn-BT can be used as candidate buffer material at soil pH. However, at a higher concentration of contaminant, the sorption would have a negative effect with a declined k_d. Moreover, the sorption capacity of UCBT (5.51×10^{-3} mol/m^2) was in the range of a potent buffer candidate for waste repositories as compared to other sorbents.

Acknowledgments The author is grateful to Prof D. N. Singh for providing valuable suggestions during the course of study. The Sophisticated Analytical Instrumentation Facility (SAIF) and Nanoindentation Facility at IIT Bombay are gratefully acknowledged.

Compliance with ethical standards

Funding Agency This research did not receive any specific grant from funding agencies in the public, commercial, or not-for-profit sectors.

References

Alfredo K, Adams C, Eaton A, Roberson JA, Stanford B (2014) The potential regulatory implications of strontium. American Water Works. http://www.awwa.org/Portals/0/files/legreg/documents/2014AWWAStrontiumBriefingPaper.pdf. Accessed 06 July 2016

Arnepalli DN, Rao BH, Shanthakumar S, Singh DN (2010) Determination of distribution coefficient of geomaterials and immobilizing agents. Can Geotech J 47:1139–1148

ASTM D 5550–06 (2008) Standard test method for specific gravity of soil solids by gas pycnometer, Annual Book of ASTM Standard, 04.08, ASTM, Philadelphia, USA

Caglar B, Afsin B, Tabak A, Eren E (2009) Characterization of the cation-exchanged bentonites by XRPD, ATR, DTA/TG analyses and BET measurement. Chem Engg J 149:242–248

Chegrouche S, Mellah A, Barkat M (2009) Removal of strontium from aqueous solutions by adsorption onto activated carbon: kinetic and thermodynamic studies. Desalination 235:306–318

Chen CC, Hayes KF (1999) X-ray absorption spectroscopy investigation of aqueous Co(II) and Sr(II) sorption at clay-water interfaces. Geochim Cosmochim Act 63:3205–3215

Coppin F, Berger G, Bauer A, Castet S, Loubet M (2002) Sorption of lanthanides on smectite and kaolinite. Chem Geol 182:57–68

Duman O, Tunc S (2009) Electrokinetic and rheological properties of Na-bentonite in some electrolyte solutions. Micropor Mesopor Mat 117: 331–338

Galambos M, Osacky M, Rosskopfova O, Krajnak A, Rajec P (2012) Comparative study of strontium adsorption on dioctahedral and trioctahedral smectites. J Radioanal Nucl Chem 293:889–897

Glasstone S, Dolan PJ (1977) The effects of nuclear weapons. Chapter XII, Biological Effects, III Edition, U.S. Department of Defense and the Energy Research and Development Administration, 605. http://www.fourmilab.ch/etexts/www/effects/eonw_12.pdf.

Gllowiak BJ, Pacyna J, Pallczynski RJ (1977) Strontium-90 and caesium-137 contents in human teeth. Environ Pollut 14:101–111

Guimaraes V, Azenha M, Rocha F, Silva F, Bobos I (2014) Influence of pH, concentration and ionic strength during batch and flow-through continuous stirred reactor experiments of Sr^{2+}-adsorption onto montmorillonite. J Radioanal Nucl Chem 303:2243–2255

Gumaste SD, Iyer KR, Sharma S, Channabasavaraj W, Singh DN (2014) Simulation of fabric in sedimented clays. Appl Clay Sci 91–92:117–126

Guven N (1990) Longevity of bentonite as buffer material in a nuclear waste repository. Engg Geol 28:233–247

Hancock BC, Carlson GT, Ladipo DD, Langdon BA, Mullarney MP (2002) Comparison of the mechanical properties of the crystalline and amorphous forms of a drug substance. Internat J Pharmaceut 241:73–85

He Y, Chen YG, Ye WM (2016) Equilibrium, kinetic, and thermodynamic studies of adsorption of Sr(II) from aqueous solution onto GMZ bentonite. Environ Earth Sci 75:807–817

Hong HJ, Ryu J, Park IS, Ryu T, Chung KS, Kim BG (2016) Investigation of the strontium (Sr(II)) adsorption of an alginate microsphere as a low-cost adsorbent for removal and recovery from seawater. J Environ Manag 165:263–270

IAEA (2006) The management system for facilities and activities, International Atomic Energy Agency Safety Standard No. GS-R-3, Vienna, pp 1–43.

India Energy Outlook (2015) World energy outlook special report, International Energy Agency 135, www.world energy outlook.org/india.

Kamei-Ishikawa N, Ito A, Umita T (2013) Fate of stable strontium in the sewage treatment process as an analog for radiostrontium released by nuclear accidents. J Hazard Mater 260:420–424

Karnland O, Olsson S, Nilsson U, Sellin P (2007) Experimentally determined swelling pressures and geochemical interactions of compacted Wyoming bentonite with highly alkaline solutions. Phys Chemist Earth 32:275–286

Keceli G (2015) Adsorption kinetics and equilibria of strontium onto kaolinite. Separation Sci Technol 50:72–80

Krauskopf KB, Bird DK (1995) Introduction to geochemistry, 3rd edn. McGraw-Hill, New York

Kwon S, Cho WJ, Lee JO (2013) An analysis of the thermal and mechanical behavior of engineered barriers in a high-level radioactive waste repository. Nucl Eng Technol 45:41–52

Lalikova S, Pajtasova M, Ondrusova D, Bazylakova T, Olsovsky M, Jona E, Mojumdar SC (2010) Thermal and spectral properties of natural bentonites and their applications as reinforced nanofillers in polymeric materials. J Therm Anal Calorim 100:745–749

Langley S, Gault AG, Ibrahim A, Takahashi Y, Renaud R, Fortin D, Clark ID, Ferris FG (2009) Sorption of strontium onto bacteriogenic iron oxides. Environ Sci Technol 43:1008–1014

Madejova J (2003) FTIR techniques in clay mineral studies. Vibration Spectros 31:1–10

Mckinley IG, Alexander WR, Blaser PC (2007) Development of geological disposal concepts. Radioact Environ 9:41–76

Moayedi H, Asadi A, Huat BBK, Kazemian S (2011) Zeta potential of organic soil in presence of calcium chloride, cement and polyvinyl alcohol. Inter J Electrochem Sci 6:4493–4503

Oliver WC, Pharr GM (1992) An improved technique for determining hardness and elastic modulus using load and displacement sensing indentation experiments. J Mater Resear 7:1564–1583

Oyen ML, Cook RF (2009) A practical guide for analysis of nanoindentation data. J Mech Behav Biomed Mater 2:396–407

Parkhomenkho EI (1967) Electrical properties of rocks, Springer, Planum Press, New YorkISBN–13: 978–1–4615-8611-1.

Parkman RH, Charnock JM, Livens FR, Vaughan DJ (1998) A study of the interaction of strontium ions in aqueous solution with the surfaces of calcite and kaolinite. Geochim Cosmochim Act 62:1481–1492

Pathak P (2014) Determination of distribution coefficient of soil-contaminant system. Dissertation, Indian Institute of Technology Bombay India.

Pathak P, Singh DN, Pandit GG, Rakesh RR (2014a) Determination of distribution coefficient: a critical review. Internat J Env Waste Manag 14:27–64

Pathak P, Singh DN, Pandit GG, Apte PR (2014b) Establishing sensitivity of distribution coefficient on various attributes of soil-contaminant system. J Hazard Toxic Radio Waste 18:64–75

Pathak P, Singh DN, Pandit GG, Rakesh RR (2015) Guidelines for quantification of geomaterial-contaminant interaction. J Hazard Toxic Radio Waste 20:1–10

Poernomo H (2010) Sorption and dispersion of strontium radionuclide in the bentonite-quartz-clay as backfill material candidate on radioactive waste repository. Indo J Chem 10:276–284

Seliman AF, Lasheen YF, Youssief MAE, Abo-Aly MM, Shehata FA (2014) Removal of some radionuclides from contaminated solution using natural clay: bentonite. J Radioanal Nucl Chem 300:969–979

Skupinski S, Solecki J (2014) Studies of strontium (II) sorption on soil samples in the presence of phosphate ions. J Geochem Explor 145: 124–128

Smiciklas I, Jovic M, Sljivic-Ivanovic M, Mrvicb V, Cakmak D, Dimovic S (2015) Correlation of Sr^{2+} retention and distribution with properties of different soil types. Geoderma 253–254:21–29

Smykatz-Kloss W (1982) Application of differential thermal analysis in mineralogy. J Therm Anal 23:15–44

Srinivas K, Shusha Lekshmi SU, Susmita S, Singh DN (2013) Investigations to establish the influence of the thermal energy field on soil properties. Acta Geotechnica Solvenica 2:59–76

Srivastava RR, Mittal NK, Padh B, Reddy BR (2012) Removal of tungsten and other impurities from spent HDS catalyst leach liquor by an adsorption route. Hydrometallurgy 127–128:77–83

Srivastava RR, M-s K, Lee J-c (2013) Separation of tungsten from Mo-rich leach liquor by adsorption onto a typical Fe-Mn cake: kinetics, equilibrium, mechanism, and thermodynamics studies. Ind Eng Chem Res 52:17591–17597

Till JE, Grogan H (2008) Radiological risk assessment and environmental analysis, Chapter 5, Transport of Radionuclides in Groundwater, Oxford Scholarship Online, ISBN-13: 9780195127270

Wallace SH, Shaw S, Morris K, Small JS, Fuller AJ, Burke IT (2012) Effect of groundwater pH and ionic strength on strontium sorption in aquifer sediments: implications for ^{90}Sr mobility at contaminated nuclear sites. Appl Geochem 27:1482–1491

Wang TH, Liu TY, Wu DC, Li MH, Chen JR, Teng SP (2010) Performance of phosphoric acid activated montmorillonite as buffer materials for radioactive waste repository. J Hazard Mater 173:335–342

Wendlandt WW (1975) The thermal properties of inorganic compounds, III Strontium chloride 6-hydrate. Thermochim Acta 12:359–366

Zhijian W (2008) Selection and basic properties of the buffer material for high-level radioactive waste repository in China. Acta Geolog Sinica 82:1050–1055